AIAA 93-2304
Advanced SST Auxiliary Air Intakes Design and Analysis

T. Bardagi and J.L. Lecordix
Snecma - Villaroche

AIAA/SAE/ASME/ASEE
29th Joint Propulsion Conference and Exhibit
June 28-30, 1993 / Monterey, CA

ADVANCED SST AUXILIARY AIR INTAKES DESIGN AND ANALYSIS

Thierry BARDAGI, Jean-Loïc LECORDIX
(Snecma Villaroche 77550 Moissy-Cramayel)

Abstract

Within the context of future supersonic transport propulsion, Snecma carried out a study on the variable-cycle engine aerodynamic integration. In the takeoff and subsonic flight phase, auxiliary air intakes located in the nacelle walls are necessary for the auxiliary fan air supply. This paper deals with the design and optimization of these air intakes.

Aerodynamic optimization of the air intake has been realized numerically, first by Euler 2D CFD computations and boundary layer calculations, then air intake design was performed by means of CAD and 3D Euler aerodynamic calculations. The results of these calculations were used to design the final concept.

A test scale model was designed to study several concepts in the ONERA transonic wind tunnel S3CH in Meudon. Instrumentation which analyses the aerodynamic flow included wall static pressure measurement sensors and in particular a rake for flow measurement at the engine station, fitted with dynamic sensors (Kulite) which measurements are analysed in real time.

The local aerodynamic measurements were compared with calculation results. Then global performance of the system has been displayed (efficiency and distortion data).

Nomenclature

dPRS	Loss of surge pressure ratio
$D_{ST,FAN}$	Entry corrected flow
$K\theta$	Circumferential distortion index
KRA2	Radial distortion index
M	Mach number
M_∞	Free stream Mach number
M_I	Ideal Mach number
P_S	Static pressure
P_T	Total pressure
ε	Mass flow coefficient
β	Blow-in door setting angle
$\eta_{\infty, FAN}$	Inlet pressure recovery

Subscripts

st	steady
ust	unsteady

Introduction and objectives

Concorde entered commercial service in 1976, after fifteen years of intensive research, six of which devoted to flight tests. As known the aircraft was due to prove outstandingly successful from the technical point of view, as evidenced by regular revenue service that has totalled 150,000 hours of flight so far with no accident. Although Concorde has become synonymous with supersonic transportation (SST), it has shown to be a commercial failure to some extent however due to changes air transportation business experienced in the meantime: so far only 14 Concordes have been used in service.

Concorde revenue operation will probably end toward 2005. It can reasonably be assumed that before then demands for high speed air routes will appear. The long haul traffic share is still increasing and flight stages are getting longer (14 flight hours non-stop in subsonic mode !).

To succeed two main conditions that greatly influence the propulsion system have to be met as regards this supersonic transport aircraft of the second generation.

- Cost-effectiveness that rules the objectives in terms of SFC and weight,
- Protection of the environment that imposes noise and pollutant emission limits.

Variable-cycle engine solving the noise problem

Noise levels around airports should meet the FAR Part 36 Stage 3 noise regulations. Noise levels strongly depend on gas exhaust speed. In fact it is known that high bypass ratio engines with low specific thrust and very low gas exhaust speed generate little noise. In addition, in supersonic mode a high specific thrust, i.e. an exhaust speed notably higher than flight speed, is required for the nacelle drag to be limited. A solution is to develop an engine with different cycles for takeoff and the subsonic mode on the one hand and for the supersonic mode on the other hand. All these considerations have led Snecma to define a peculiar type of variable-cycle engine (1), (2) which features a device called "airflow rate multiplier", capable of significantly increasing airflow rate suited for Mach 2 operation to the rate required for takeoff and subsonic flight.

MCV99 general architecture

The MCV99 principle relies on a basic single-spool engine for supersonic operation, with at its smallest cross-section (i.e. at the HP compressor outlet, an auxiliary peripheral fan fed by a secondary air inlet that

allows the airflow rate to be significantly increased for ensuring sufficient thrust and reduced exhaust speed at takeoff. The fan is driven by high pressure air bled at the engine outlet. It is used at takeoff in order to limit noise. Then in high subsonic mode and in transonic mode, the auxiliary air intakes are closed and the secondary flowpath is sparingly supplied with excess air from the primary air intake. In supersonic mode, finally, the engine operates on a single flow, the secondary flowpath being used only to evacuate air coming from the primary air intake boundary layer bleed. Such a configuration has the advantage of operating on dual flow at takeoff and on single flow single spool in supersonic mode (Fig. 1). As a result the variable-cycle engine concept, as illustrated by Snecma MCV99 project, can provide at the same time moderate specific fuel consumption in subsonic and supersonic mode, low noise at takeoff and reduced emissions of nitrogen oxides.

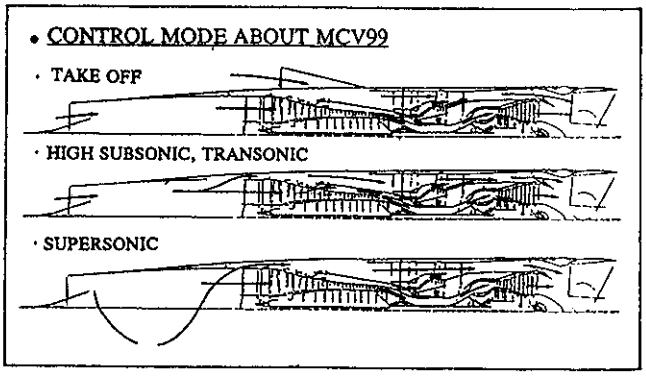

Figure 1 : MCV99 engine architecture

Efficiency and distortion specifications

In order to maintain the level of thrust over the flight track Snecma Project Design has estimated the efficiency variations to be complied with at maximum fan rating up to closing of the secondary air intakes (fig.9).

One major concern in compressor and particularly in fan operation is the prevention of stall that is promoted by several parameters, among which flow heterogeneity at engine inlet that plays an essential role. Integrating a fan behind a complex supply system entails additional risks that have to be detailed. This is why a detailed study on the admissible distortion levels in the engine has been conducted.

. To prove the auxiliary air intakes system is reliable, we have applied ourselves to designing a system fitted with a fan having surge margin data comparable with those in conventional commercial engines. According to Snecma's long experience based on CFM56 family engines tests, the surge margin consumption due to distortion is around 10% at maximum rating and it has been our objective when dimensioning the air intakes.

Fan sensitivity to distortion has been determined by means of an extensive numerical study. The LABICHE code (3) used for solving the Euler 3D equations for all compressor stages with flow heterogeneities allowed for has been applied to the MCV99 fan by imposing a total pressure distortion level at engine inlet. Calculating the consumed margin from the stability loop makes possible to predict the fan distortion sensitivity $\frac{d\,\mathrm{Pr}\,s}{K\theta_{ust}} = 0.13$

Then, after taking into consideration all these results and the distortion progression required as a function of rating, based on Snecma's experience, the limit unsteady distortion curve not to be exceeded when designing the secondary air intakes has been determined.

Design

Air supply to the engine fan through secondary air intakes has the following characteristics:
- Separation of primary and secondary tasks, i.e. no supply to the fan through the primary air intake.
- Operation in the subsonic range up to $M\infty = 0.66$ and up to the maximum flow rate,
- Supply through large openings located on the nacelle walls,
- Openings on the lateral sides and lower sides, no opening on the upper side due to the wing.
- Air intake all-or-nothing operation.

Solutions inventory

Several possible concepts have been analysed to evaluate aerodynamic performance (efficiency, distortion and drag) in subsonic phase. Three main air supply principles have been retained (Fig. 2):
- scoop intake,
- blow-in doors intake,
- flush intake (two configurations are possible, one with parallel walls, the other with divergent walls such as the NACA air intake).

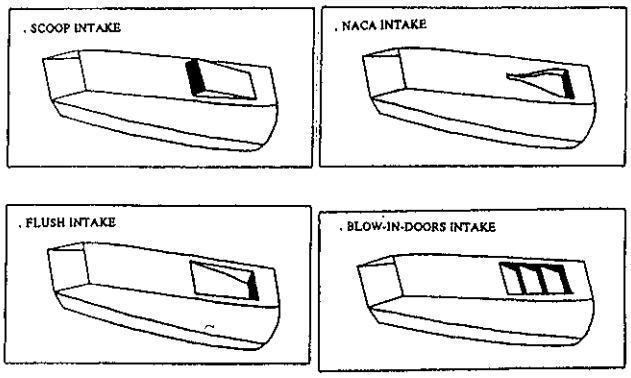

Figure 2 : Auxiliary air intakes possible concepts.

The parametric study was concerned with the following items (see Fig. 3):
- nacelle-diffuser connection area (opening forward zone, see detail A Fig. 3),
- internal wall contour (diffuser lines),

- quantity of doors,
- introduction of flow guide vanes downstream of the doors,
- rotation points,
- rotating angles and length of doors,
- profile pressure face shape, suction face shape imposed by nacelle lines.

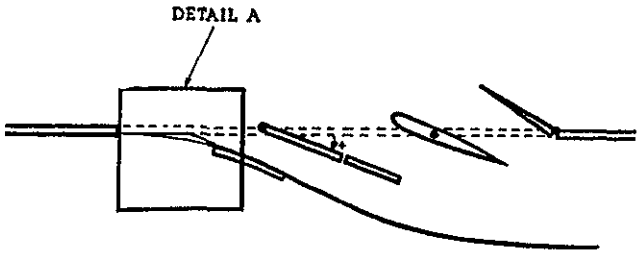

Figure 3 : Geometric degrees of freedom

Numerical methods

In order to reduce the number of tests and costs thereof, Snecma has built a numerical methodology that allows the flow fields around complex geometries to be calculated. To do so, 3D mesh generation software programs (MESH3D[4], OPTIM3D[5]), 3-D Euler codes (SESAME[6], [7], [8], FLU3M[9], [10], [11]) and boundary layer codes (integral method[12], 3C3D[13]) are used. The codes MESH3D, OPTIM3D, SESAME and FLU3M have been developed by ONERA and industrialized by Snecma. Plane and surface meshes are obtained using CATIAMESH that proceeds from the CATIA system.

2-D meshes

The SESAME code was used for the 2-D numerical analysis. The multidomain approach of the SESAME code proves extremely convenient. In the case of complex geometry it allows breakdown of the calculation domain into several zones topologically and numerically independent. In the global calculation the zones are linked to one another due to connection boundary conditions based on the compatibility relation method. The SESAME code can deal with interfaces between two zones even if there is no node cross-reference, with the two zones overlapping each other in some cases. The complete meshes used for this part are composed of a sequence of 5 identical 2-D plane meshes being parallel. H type2-D meshes mainly have been generated (C type meshes are used to discretize the calculation domains close to thick profiles, in particular, scoop leading edges). The complete meshes include 80,000 nodes.

3-D Mesh

The 3-D aerodynamic numerical study has been carried out using the FLU3M calculation code. Mesh discretizes nacelle fitted with 4 flush air intakes(Fig. 4). This evolved mesh includes 20 H-meshed zones with no nodes coincidence between certain zones. 540,000 nodes were required to describe at best and with accuracy geometrical complexity, in particular nacelle thicknesses and joining radii between the diffuser wall and the upper pylon.

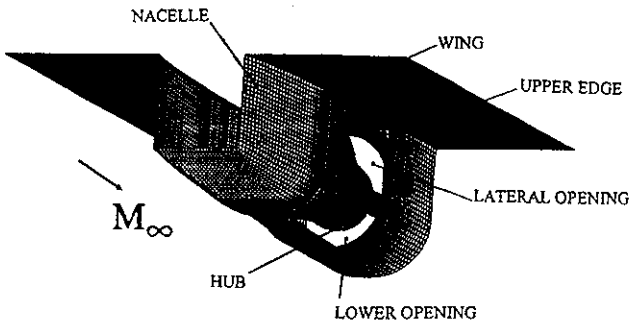

Figure 4 : Basic concept mesh - Wall surfaces

Air intake concepts

NACA air intake

This type of air intake has been studied by JELL C.S. [14] and Charles F. Hall [15]. An interesting result is related to the NACA type air intake that shows good efficiency (comprised between 0.90 and 0.95) as long as the flight Mach number remains below 0.9 and drag is low, provided the two geometrical criteria hereafter are met:

α = 7 degrees (divergence angle) ; l/h = 4

where l and h are the length and height of the opening aft cross-section.

Introducing a NACA concept that meets these two criteria caused size problems as regards length and depth, so that the solution was not selected as part of the project.

Scoop air intake

The goal was to examine the feasibility of such a concept and carry out a preliminary study in order to define the diffuser aerodynamic lines. The parametric analysis included the following assumptions:

- external compression in order to limit separation hazards within the diffuser. The optimization criterion relies on making sure front cross-sections between the scoop leading edge and the fan evolve uniformly (one dimensional study),
- low flow rate coefficient ε = 0.83 at $M\infty$ = 0.66, selected on an external compression basis
- selection of 2 side scoops with 12° aperture angle

The following results were obtained:

- external separation and high drag were highlighted by a 2-D Euler calculation with this geometry.
- Integrating relative pressures into these large-size scoops leads to very high loads and technological dead end as a result.

Due to the results of the study the scoop project has been dismissed.

Flush concept

A 2-D numerical study using the SESAME code has been carried out on the flush concept. It aimed at optimizing the diffuser inner line, in particular, to the influence of the contour that links the nacelle with the internal diffuser wall.

Flush concept with slope discontinuity leads to an ideal peak Mach number on the wall to 1.221. Thus, it is to be feared that some separation flow could occur downstream in the hub and could generate supplemental drag.

After optimizing the diffuser internal line, the effect of slope continuity makes the ideal peak Mach number on the wall decrease to 0.882.

Numerical analysis of the flush configuration featuring slope continuity between nacelle and diffuser internal flow path and complemented by a boundary layer calculation yields quite good results from any point of view (diffuser inlet peak Mach number reduced, the high downstream recompression of which does not induce any boundary layer separation).

Blow-in doors intake

A lot of 2-D Euler calculations have been performed with a flight Mach number of 0.66, using mesh with 40,000 to 90,000 nodes depending on configuration. Calculations were aimed at providing a qualitative analysis of the differences and determining the risks of the principle not operating (separation, shocks on nacelle contours, on doors leading edge, etc.). The study is mainly valid in the aperture upstream zone and in the doors zone where the 3-D effects are lower.

The blow-in door solution may also lead to satisfactory results, provided each door's location, setting and shape are optimized. Such optimization has been partly carried out in this study and was used as a basis for model definition. The best result is presented in Fig. 5. However it shall be noted that multiplying the number of doors makes the optimization more intricate without yielding better results.

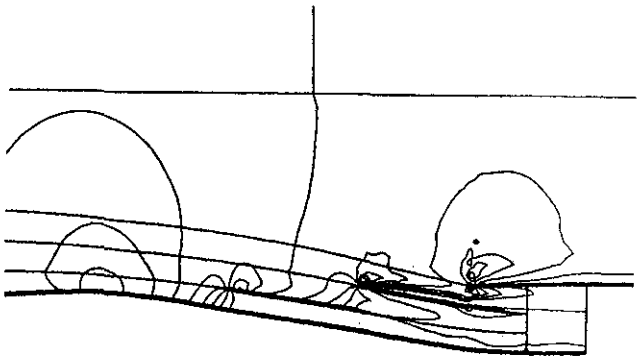

Figure 5 : 2-blow-in-door concept -M_∞ = 0.66
Mach number contours - Euler 2D calculations

Diffuser 3-D design

The previous aerodynamics study has led to selecting a basic geometrical arrangement to be tested and 4 openings have been introduced on either lateral side and lower surfaces of the nacelle.

The calculations have shown that the mean angle of attack of the stream line, on the downstream leadindg edge of the opening, is 15 degrees. The rough surface has been derived after the length of each aperture was assumed to be equal to 2 meters approximately.

The 3-D drawing of the fan supply diffuser has been completed by CATIA. Geometrical optimization and the one dimensional aerodynamic preliminary study have been developed referring to the flush intake solution with smooth junction beeween diffuser inner and nacelle walls (referred to as "basic solution"). Installing the pylon (necessary to accomodate the engine accessories) located on the diffuser upper part has been designed so as to prevent "wide separation" zones. The nacelle fitted with 4 openings is shown in Fig. 6.

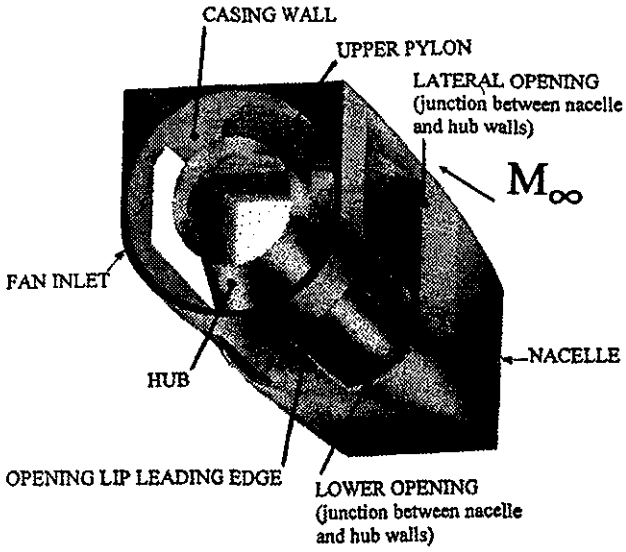

Figure 6 : Basic flush intake aft-looking view

Flush intake concept 3-D calculation

3-D Euler calculations have been carried out with FLU3M on a half nacelle (due to symmetrical geometry along a vertical plane going through the engine centerline) on one of the concepts selected (flush intake) and have allowed some defects of the model to be corrected before it is realized. Processing subsonic inlet, outlet and wall boundary conditions is based upon the compatibility relations method. Connecting conditions are processed by fictious node interpolation, ensuring conformance to the scheme sequence. Slip conditions have been imposed on the walls (see Fig. 6). The total pressure, total temperature and direction of flow are imposed on the subsonic upstream interface. The free stream static pressure and the fan inlet static pressure are respectively imposed on the subsonic downstream boundary and on the fan inlet boundary. The fan boundary inlet pressure is calculated from the flow rate

desired and uniformly distributed. A non-reflecting condition is applied to the domain external interface that symbolizes infinite.

The complete numerical analysis of the basic configuration (see Fig. 4 and 6) was carried out at 0.66 flight Mach number and with different engine flow rates. 25,000 explicit calculation iterations were required to achieve satisfactory convergence. Fig. 7 showing the Mach number distribution over the walls for maximum corrected fan mass flow highlights the following design problems:
- diffusion too high downstream of the pylon,
- pronounced overspeed zone at the upper edge in casing wall.

Separation on the pylon is indicated by a calculation using tridimensionnal boundary layer code from the latter result. Shape could not be corrected on the model before it was realized. A more detailed analysis where test results are compared with calculation is presented later here.

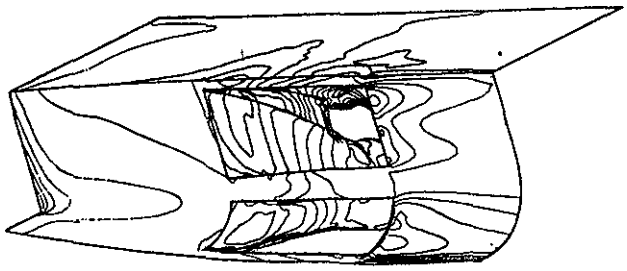

Figure 7 : Basic configuration 3D Euler calculation. IsoMach number contours at $M_\infty = 0.66$ and max engine massflow.

Experimental results

Test facilities

Model principle and scale

The model has been installed on the side wall of the ONERA S3CH wind tunnel in Meudon. Cantilever assembly is specific to the air intakes studies and features a venturi tube for initiating suction and measuring conditions thereof. The flow sucked is the air intake secondary flow. The primary flow is the natural flow driven backwards. Primary air intake flow rate not being representative, the upstream part of the air intake has been modified (thick elliptical leading edges) in order to limit separations at the external lips likely to distort downstream measurements.

The second point concerns the selection of the model scale which was chosen as large as possible, i.e. 1/8, in order to limit Reynolds deviations.

Test configuration

The modular arrangement of the model provides for geometrical configuration changes for the same concept. Fairly deep geometrical changes are also possible in changing some parts. 5 configurations have been tested:
Configuration #1: Flush concept with slope continuity between the nacelle wall and the internal diffuser wall, also called "basic concept" (fig. 8).
Configuration #2: Basic flush concept with slope discontinuity between the nacelle wall and the internal diffuser of each opening, also called "slope breaking concept".
Configuration #3 - Basic flush concept with 3 internal drip fences integrated between each opening, also called "drip fence concept".
Configuration #4 - Basic concept with 2 variable angular setting blow-in doors for each opening, also called "2-blow-in-door concept".
Configuration #5 - Same configuration as above with the upstream blow-in doors having been removed, also called "1-blow-in-door concept".

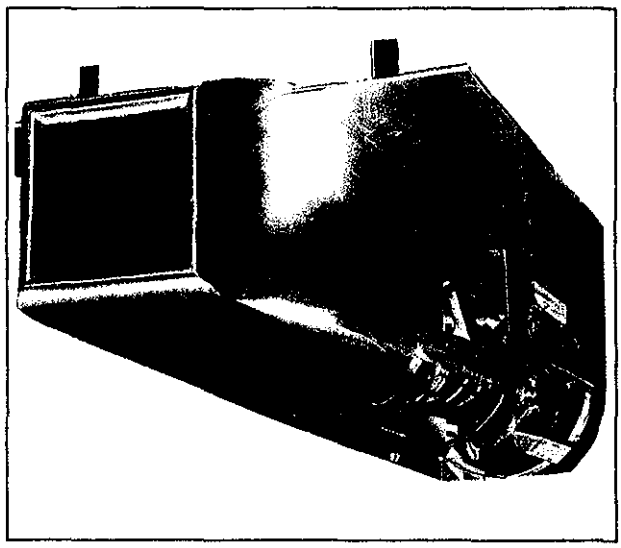

Figure 8 : Scale model - Basic configuration.

Instrumentation

Air intake efficiency ($\eta_{\infty,\ FAN}$) and transient distortion measurements (K_θ, KRA2) have been carried out. Using 8 rakes of 4 pressure probes on each. Stationary and transient measurements have been conditioned by ONERA and recorded and analysed by Snecma in real time with the CATI system[16] (Chaine d'Acquisition et de Traitement de l'Instationnaire) that provides full coverage of the air inlet/compressor interface plane.
$K\theta$, KRA2 and $\eta_{\infty,\ FAN}$ indexes are defined in the appendix.

106 wall pressure taps (24 of which on the blow-in doors) have been installed on only one side of the model in order to carry out a local analysis.
A 5-week aerodynamics test run has been realised in the ONERA S3-Ch wind tunnel in Chalais-Meudon. Equipping the air flow path and adjusting the deformable walls have been completed within 2 weeks.

Test results

Analysis of flush solutions

Fig. 9, 10 and 11 show a parabolic variation for efficiency and for the unsteady distortion index $K\theta_{ust}$ $KRA2_{ust}$ expressed as a function of the flight Mach number at maximum engine flow rate. The optimum point is located in the vicinity of Mach 0.3 - 0.4. The tests have shown that efficiency decreases with the flow rate increasing at static condition, whereas it increases at Mach 0.66. At any Mach number, distortion slightly decreases when flow rate increases. It is noted that the 3 flush configurations give very close results. Distortion measurement results remain below limits acceptable for the fan over the whole operating range. However distortion is sensitive in static conditions (between 40% and 60% in unsteady values,between 20% and 25% in steady values). Efficiency results exceeded expected levels.

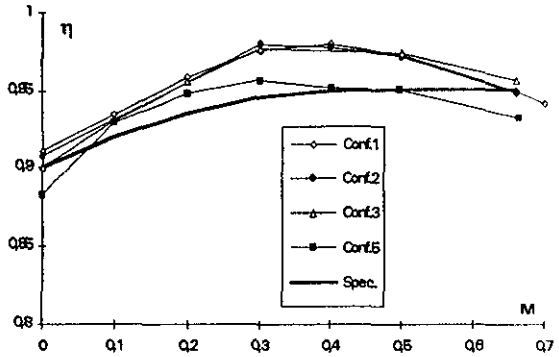

Figure 9 : Efficiency at maximum engine airflow rate

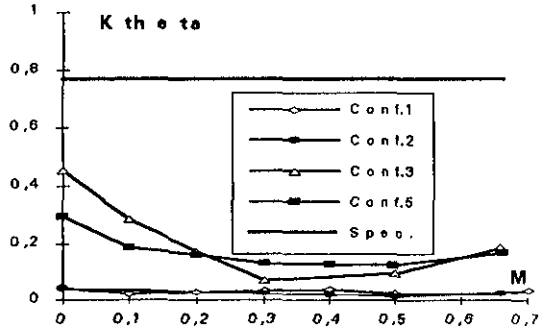

Figure 10 : Kθ at maximum engine airflow rate

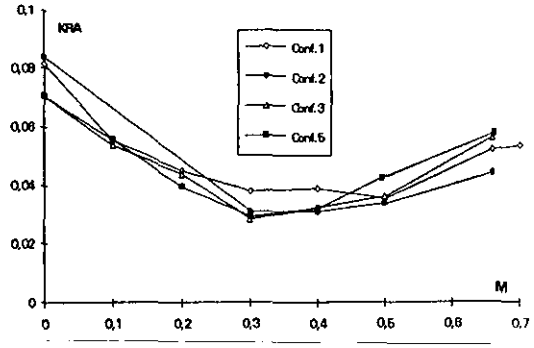

Figure 11 : KRA2 at maximum engine airflow rate

At static condition the observations made are as follows:
- Unsteady total pressure charts at maximum airflow rate in Fig. 12 indicate high total pressure loss in the downstream zone of the lower openings. Ideal Mach number local analysis reveals a much more pronounced wrapping around the leading edge of the lower opening lips (very high local acceleration) than on the lateral opening ones. Moreover, the maximum peak ideal Mach number has undoutedly not been localized. As a result, a significant shock with separation is highly probable in this zone. This assertion has been verified by visualization using sludge for the basic configuration at maximum engine airflow rate.
- Analyzing the measurements taken at the upper corner shows a maximum peak ideal Mach number in excess of 1.1 at maximum engine airflow rate.

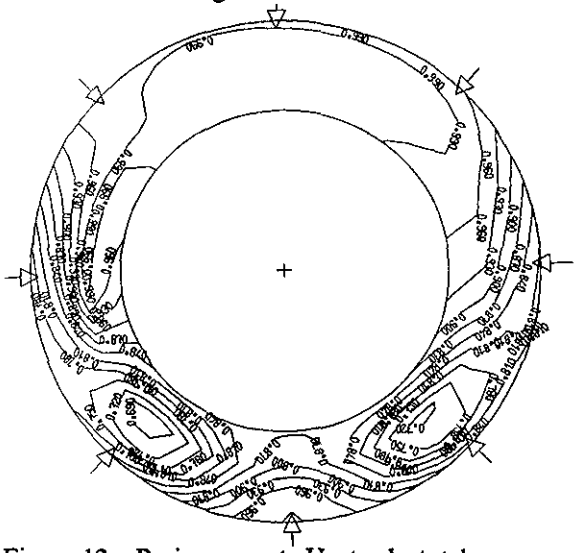

Figure 12 : Basic concept -Unsteady total pressure map *Static condition , max engine massflow.*

At 0.66 flight Mach number we note that:
- efficiency has improved thanks to the drip fences,
- unsteady total pressure charts read out at maximum engine airflow rate in Fig. 13 show for the 3 concepts significant losses in the downstream zone of the upper pylon. On the other hand, we note the separated flow between the openings has reduced due to the drip fences.

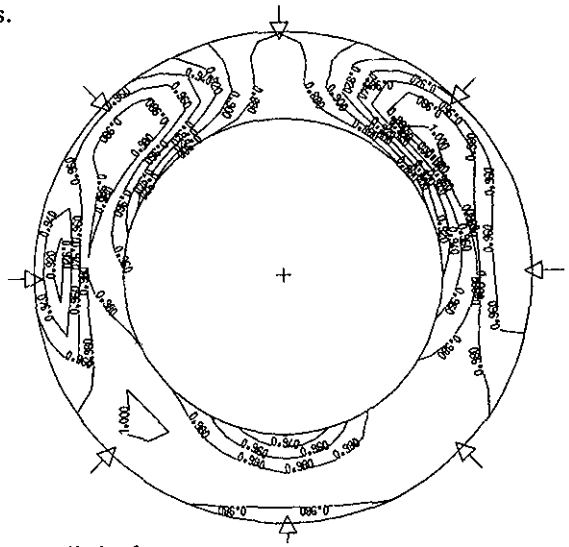

Figure 13 : Drip-fence concept -Unsteady total pressure map - M_{∞}= 0.66 , max engine massflow.

- visualization performed at maximum airflow rate clearly highlights separations on the upper pylon. This separation occurs in the joining radius between pylon and hub walls as well as in the pylon trailing edge. However no separation has been noted on the diffuser at the lower opening side. These results have actually been predicted numerically by tridimensionnal boundary layer calculation.

Let us compare the local results (ideal Mach number) for the basic configuration with the 3-D Euler numerical calculation. The aerodynamics conditions are as follows:

- Flight Mach number = 0.66
- maximum value of corrected fan mass flow (cycle data)

Ideal Mach number distributions along 2 wall lines going through the side opening, on the one hand, and the lower opening on the other hand, via the nacelle and the internal diffuser, are plotted in Fig. 14a and 14b. It is noteworthy that in each case the results show good agreement and there is no critical zone (no separation risks).

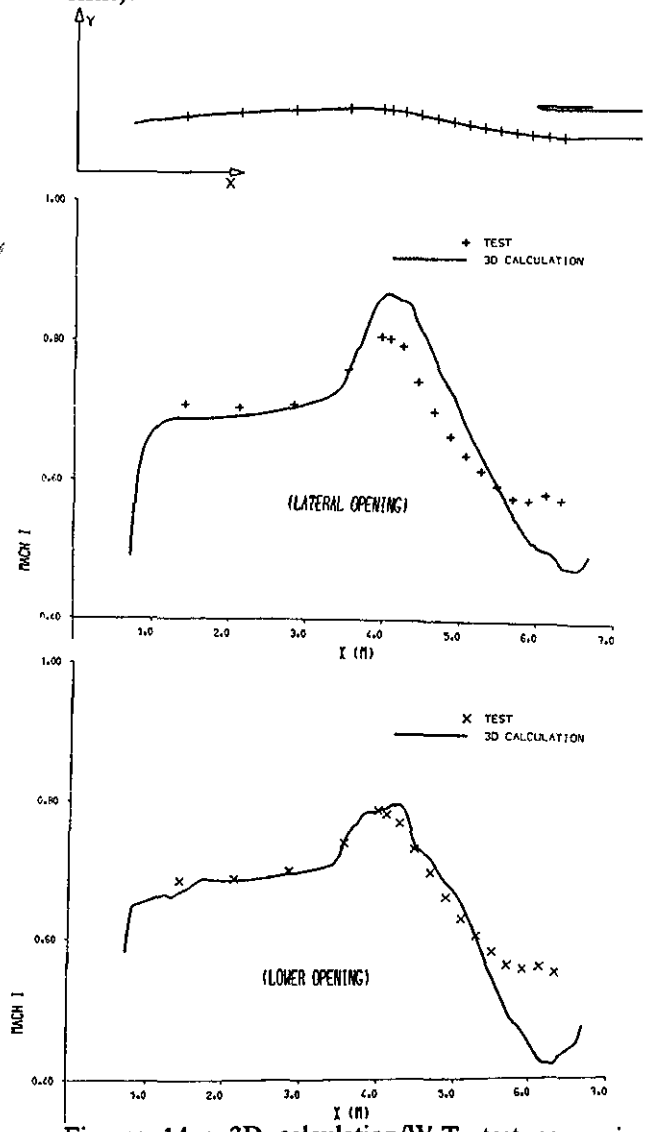

Figures 14 : 3D calculation/W.T. test comparison - Ideal Mach number distribution
M_∞ = 0.66 , max engine massflow.

If we analyse the ideal Mach number distribution downtream the leading edge of the side opening, the results also show good agreement. The stagnation point is located at the pressure side of the lip, very close to the leading edge. The pressure side and suction side, downstream of a reasonable peak Mach number ($\leq$ 0.75), deceleration is slight.

Ideal Mach number distribution on a wall line going along the pylon is plotted in Fig. 15. Predictions using numerical calculations are comparable to the tests as long as no separation occurs. Downtream of this location separation is governed by viscous effects and the Euler calculation has no physical significance any longer.

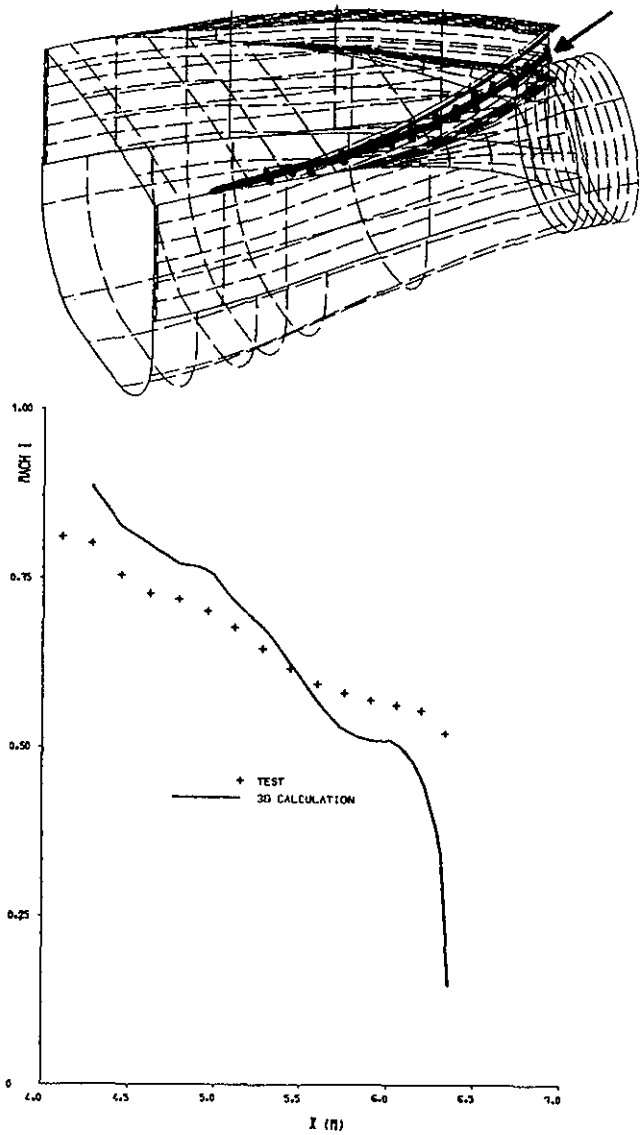

Figure 15 : 3D calculation/W.T. test comparison - Ideal Mach number distribution along the pylon
M_∞ = 0.66 , max massflow.

Finally, there is good prediction of the ideal Mach number at the upper edge where the peak Mach number is severe ($\geq$ 0.8) for this air flow rate (Fig. 16). At maximum engine airflow rate, the peak ideal Mach number is in excess of 0.8 for all flight Mach numbers.

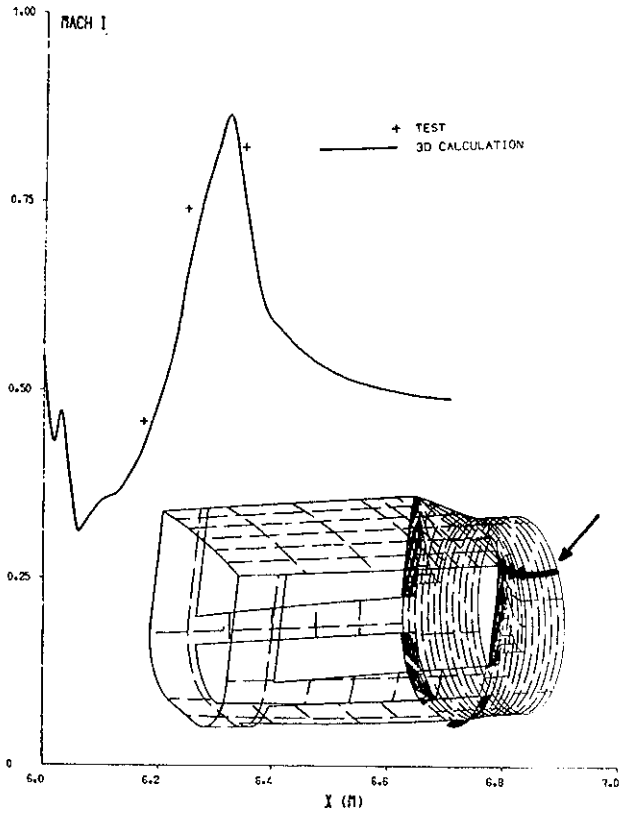

Figure 16 : 3D calculation/W.T. test comparison - Ideal Mach number distribution along the upper edge.
$M_\infty = 0.66$, max massflow.

Test data analysis of the flush concepts show some performance penalties due to some design features. Improvements that can be envisaged to remedy it are as follows:
- the casing lips internal contraction ratios must be increased to reduce overspeed at static condition;
- the drip fences located between the different openings are required as a result. Their shapes must be subjected to detailed studies and optimized;
- the pylon must ensure smoother axial distribution of the slope (more particularly in the vicinity of the trailing edge);
- joining radius between hub and pylon walls must be increased;
- the upper corners must have a slope axial distribution less severe.

Taking into account the wall boundary layer penalty (approximately 1% on efficiency) and the benefics of the above imprevements, the efficiency for the drip fence concept will be at maximum engine airflow rate in excess of 0.96 in the flight Mach number range between 0.3 and 0.66.

Analysis of blow-in doors concepts

Variations in efficiency and in the distortion index KΘ, KRA2 expressed as a function of the flight Mach number at maximum engine airflow rate are given in Fig. 9, 10 and 11. The general shapes of the curves remains unchanged.

At static condition the lessons learned are as follows:
- efficiency results for the configuration with one blow-in door are similar to the flush concepts. On the contrary a slight efficiency penalty for the best configuration fitted with two blow-in doors and 15° aperture is noted.
- Distortion results are satisfactory and much better compared to the flush concepts. This is due to the fact that the doors favour smoother longitudinal supply through the openings since the flow is guided. Unsteady total pressure charts (Fig. 17) show that losses noted for flush concepts downstream of the lower openings are no longer visible. The airflow being sucked in a smoother way through the working passage of the lower opening, air flow turning around the leading edge of the lips is less severe. Losses due to shock and separation at the pressure side are lower compared to flush concepts.

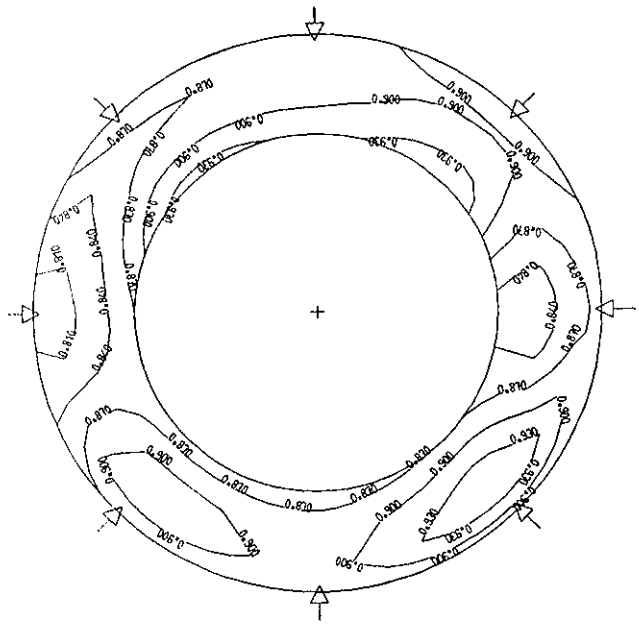

Figure 17 : 2 blow-in doors and 15° aperture concept - Unsteady total pressure map - static condition, max engine massflow.

At 0.66 flight Mach number the results are:
- the 2 blow-in door configurations lead to efficiency penalty due to the reasons below:
  * shock at the pressure side and suction side of the blow-in doors
  * flow blockage at high airflow rate
  * wetted surfaces generating wakes

- the one-blow-in-door configuration shows a slight efficiency penalty compared to the flush concepts. Performance data achieved become a little less than originally expected.
- distortion measured for blow-in doors concepts is identical with that of flush concepts.
- unsteady total pressure charts (Fig. 18) show that for all configurations losses are concentrated in the zone downstream of the upper pylon.

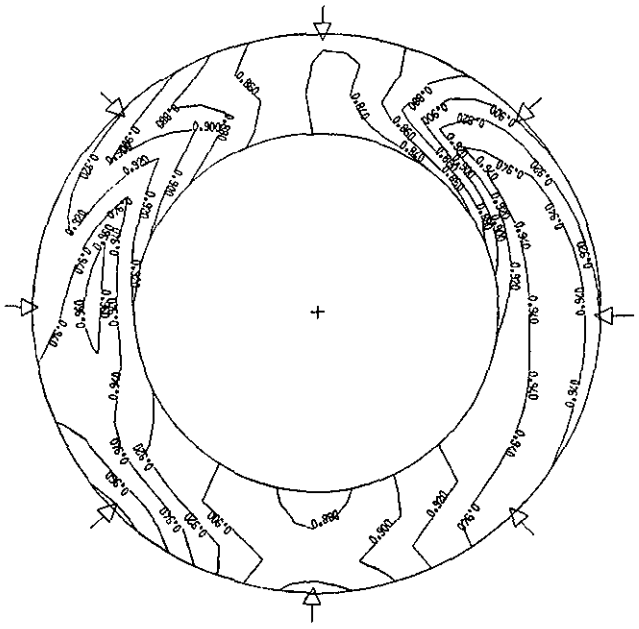

Figure 18 : 2 blow-in doors and 15° aperture concept - Unsteady total pressure map - M_∞= 0.66, max engine massflow.

Finally for all flight Mach numbers and at maximum engine airflow rate, the peak ideal Mach number measured at the upper corner located between the side opening and the fan is of the order of 1 (it is in excess of 10% for the 2-blow-in-door concept compared to the one-blow-in-door concept).

The defects listed for the flush concepts are also more or less pronounced as far as the blow-in doors concepts are concerned. Consequently the required improvements listed above are also needed for this type of concept.

The configuration with only one blow-in door seems most encouraging. In addition some doors parameters should be optimized, in particular around Mach 0.6, in order to increase efficiency.

- location of the axis of rotation on the nacelle and on the blow-in door,
- angular settings,
- lengths,
- thickness laws.

Conclusion

As part of the studies on the propulsive system intended to equip a future supersonic transportation aircraft design and optimization of secondary air intakes to supply the fan in an MCV99 type variable-cycle engine in subsonic mode up to M∞ = 0.66 have been launched on the basis of the specifications provided by Snecma Project Design.

First qualitative 2-D numerical and technological bibliographic reviews enabled us to identify various feasible concepts (flush and blow-in door secondary air intakes).

The design and engineering drawing of the model fitted with 4 openings distributing over the nacelle side and lower surfaces as well as the whole instrumentation have been completed using CATIA. Optimization has been numerically carried out using the Euler 3-D FLU3M code and was not completed at the time the tests model was constructed.

An aerodynamics test run has been completed in the ONERA S3-Ch wind tunnel at Chalais-Meudon.

The global performance test results are as follows:

- the flush configurations provide good efficiency, slightly better than expected, near 0.96 at cruise (for drip fence concept);
- distortion is moderate and less than the fan tolerances;
- as far as blow-in doors are concerned, efficiency results are not so good, however distortion is low over the whole operating range.

Local analysis of wall pressures complemented by 2 visualizations using sludge in the case of the basic flush concept at maximum engine airflow rate, on the one hand at static condition, on the other hand at 0.66 flight Mach number has highlighted the following features:

- diffusion donwstream of the upper pylon too severe,
- opening lip leading edge too thin,
- upper corners must a slope axial distribution less severe,

which call for future improvements that could easily be included in a future project.

Good performance data obtained with the study allow to conclude that the secondary air intakes concept which is part of the supersonic aircraft project equipped with variable-cycle engines is aerodynamicaly reliable.

Acknowledgements

This study has been conducted at Snecma Engineering. The authors are grateful towards the Direction des Programmes de l'Aviation Civile (DGAC/DPAC) for funding this study and STPA for technical control. We also express our thanks to Snecma, particularly to Mr. Joël XICLUNA and Mr. Alain CHOISEAU, the CATI specialists as well as ONERA (especially Mr. Bernard MAURY, Mr. Claude SANS, Mr. Rémy THEPOT and Miss Anne LECHEVRANTON). We also express our thanks to Snecma General Management and to DGAC for authorizing this publication.

References

(1) MENIOUX C. - AGARD 1979 - Cycle Variable et Transport Supersonique - Snecma

(2) HABRARD A. - The variable-cycle engine - A solution to the economical and environment challenge of the future supersonic transport - Snecma.

(3) H. JOUBERT - Flowfield calculation in Compressor Operating with Distorted Inlet Flow ASME - June 11-14, 1990 - Brussels - Belgium.

(4) F. MONTIGNY-RANNOU,
O.P. JACQUOTTE
MESH3D: un outil pour la construction des maillages tridimensionnels
AAAF - 29ème Colloque d'Aérodynamique appliquée - C.E.L. - Biscarrosse (France) 21-23 septembre 1992.

(5) O. P. JACQUOTTE
Recent progress on mesh optimization
Third international conference on numerical grid generation in computational fluid dynamics - Barcelona - Spain June 3-7, 1991.

(6) A.M. VEUILLOT
A multi-domain 3D Euler Solver for flows in Turbomachines
Proceedings of the 9th ISABE Symposium edited by F.S. Billig, AIAA, Washington D.C., Sept. 1989.

(7) V. COUAILLIER
Application du code SESAME aux calculs d'écoulements tridimensionnels de fluide parfait - discussion technique du 26 juin 1990 - ONERA.

(8) R. PEYRET
Résolution numérique des systèmes hypersoniques. Application à la dynamique des gaz- Publication ONERA 1977 - 5.

(9) Ph. GUILLEM, M. DORMIEUX
Design of 3D multi-domain Euler code
International Seminar on Supercomputing, Boston (USA), 3-5 Oct., 1989.

(10) G. ROLLIN, M.BORREL, PH. GUILLEM, J. L. MONTAGNE
Numerical Simulation of Complex three-dimensional Flows by an upwing Euler method.
IMACS, Paris, 18-22 juillet 1988.

(11) G. FRESKOS, O. PENANHOAT
Numerical simulation of the flow field around supersonic air intakes - ASME, 30 septembre 1992.

(12) PAPAILLIOU, K. D.
Optimisation des dispositifs décélérateurs à forte charge fondée sur une théorie intégrale de la couche limite.
Thèse de Doctorat et Sciences Univ. de Lyon, 1974.

(13) R. HOUDEVILLE - C. MAZIN
Calcul de couches limues tridimensionnelles par une méthode des caractéristiques ONERA (CERT), mars 90.

(14) JELL C.S.
Air Intake Aerodynamics - British Aerospace Plc. AGARD Report N° 754

(15) CHARLES F. H ALL and F. DORN BARCLAY
An experimental investigation of NACA submerged inlets at high subsonic speeds - Inlets forward of the wing leading edge - National advisory committee for aeronautics - Washington - June 9, 1948

(16) EYRAUD J. L. and AUZOLLE F.
Unsteady pressure data acquisition and processing in air inlet flow distortion surveys - Royal Aeronautical Society Forum, Bath (U.K.) April 1989.

(17) Inlet total pressure distortion considerations for gas turbine engines - AIR N° 1419 SAE, May 1983.

Appendix

Characterization of distortion indexes

A number of criteria have been proposed and are now used by the engine and aircraft manufacturers [17] to characterize the mapping of total pressure that supplies the engine.

For this purpose Snecma has used several types of distortion index, with the best results obtained with the Kθ, KRA2 indexes. Therefore only these results are presented here.

On the basis of instrumentation featuring 4 sensors with 8 rakes distributed every 45° the Kθ and KRA2 indexes are defined as follows:

$$K\theta = \frac{\sum_{j=1}^{4} K\theta j \times \frac{1}{Rj}}{Q \sum_{j=1}^{4} \frac{1}{Rj}}$$

where
Rj = ring radius

$$K\theta j = \operatorname{Max}_{n=1}^{4} \frac{(Ajn)}{n^2}$$

$$Ajn = \sqrt{(aj^2_n + bj^2_n)}$$

$$aj_n = \frac{1}{8} \sum_{i=1}^{8} Pij \cos(in\Delta\Theta)$$

$$bj_n = \frac{1}{8} \sum_{i=1}^{8} Pij \sin(in\Delta\Theta)$$

Q = steady state dynamic pressure in the measurement plane.

$$KRA2 = \frac{\sum_{j=1}^{4} (\bar{P} - Pj) \frac{1}{Rj}}{Q \sum_{j=1}^{4} \frac{1}{Rj}}$$

where $\bar{P}$ = map mean pressure

and $\overline{Pj}$ = mean pressure on ring j.

The KΘ index is based on a Fourier expansion of the total pressure of each ring, it assigns a weight reciprocally proportional to the harmonic rank. Moreover circumferential distortion is weighted by the radius reciprocal so that distortion located at the compressor hub be more significant than distortion at tip.

The KRA2 index is a radial distortion indicator. In the same way as for the KΘ index radial distortion index of each ring is weighted by the radius reciprocal.

These two indexes are made dimensionless by the steady state dynamic pressure in the plane of measurement so that these indexes be little sensitive to engine airflow rate variations.

Efficiency characterization

The total pressure loss has to be determined to allow the secondary air intake efficiency to be characterized. The air intake efficiency is defined by:

$$\eta_{\infty,FAN} = \frac{PT_{FAN}}{PT_{\infty}}$$

Thanks to the four stagnation pressure pick-ups located on each of the 8 struts of the steady state rakes, the total mean pressure can be calculated in the plane of the fan on the basis of the arithmetical mean, namely:

$$PT_{FAN} = \frac{1}{32} \times \sum_{i=1}^{4} \sum_{j=1}^{8} PT_{i,j}$$

The disadvantage of this calculation lies in this, that it provides optimistic efficiency values. Since the wall in the plane of the fan is instrumented with static pressure pick-ups a second expression of the total pressure in the plane of the fan can be derived that is more realistic. In assuming the following two detrimental hypotheses:

- the boundary layer thickness is equal to the distance d between the sensor located nearest to the wall and the wall.
- the boundary layer total pressure variation law is of Blasius type:

$$PTj(r) = [PTj(r=d) - PTj(r=0.)] \times \left(\frac{r}{(d)}\right)^{1/7} + PTj(r=0.)$$

where j varies from 1 to 8 depending on the strut, r varies from 0 to d [0, d]

the total pressure mean value $\overline{PTj}$ for each strut j is derived and, finally, the mean total pressure in the plane of the fan from the arithmetical mean:

$$PT_{FAN} = \frac{1}{8} \times \sum_{j=1}^{8} \overline{PT_j}$$